



Year: 2012

“Chiral-at-Metal” Hemilabile Nickel complexes with a latent d10-ML2 Configuration: Receiving substrates with open arms

Linden, Anthony ; Llovera, Ligia ; Herrera, Julio ; Dorta, Reto ; Agrifoglio, Giuseppe ; Dorta, Romano

Abstract: Complexes with highly reactive stereogenic metal centers are of great interest to asymmetric synthesis. Thus, by reacting $[\text{Ni}(\text{COD})_2]$ with 2 equiv of the P-alkene ligand (S)-5 ((S)-(+)-N-(3,5-dioxa-4-phosphacyclohepta[2,1-a;3,4-a]dinaphthalen-4-yl)dibenz[b,f]azepine) or (SP,SC)-6 ((2S,5S)-(-)-N-(aza-3-oxa-2-phosphabicyclo[3.3.0]octan-4-on-2-yl)dibenz[b,f]azepine), the diastereomerically and enantiomerically pure tetrahedral complexes $(\Delta, \text{S}, \text{S})\text{-}[\text{Ni}(\text{5-P}, \text{2-alkene})_2]$ (2a) and $(\Delta, \text{SP}, \text{SC}, \text{SP}, \text{SC})\text{-}[\text{Ni}(\text{6-P}, \text{2-alkene})_2]$ (2b) were obtained in almost quantitative yields on multigram scales. The Ni atoms showed in both cases stable Δ configurations. Even though these Ni(0) complexes were air stable in the solid state, once dissolved, complex 2a readily activated CS_2 , alkynes, and enones as the formal d10-ML2 fragment $[\text{Ni}(\text{5-P})_2]$ (4) to form adducts 8–11. This is possible thanks to the decoordination of the hemilabile alkene arms of the P-alkene ligands, and the X-ray crystal structures of the CS_2 and 4-ethynyltoluene adducts confirmed the 2 coordination modes of the substrates and the concomitant opening up of the alkene arms of ligand 5. The coordination of π -unsaturated carbonyl compounds in complexes 11a–c was reversible.

DOI: <https://doi.org/10.1021/om300484z>

Posted at the Zurich Open Repository and Archive, University of Zurich

ZORA URL: <https://doi.org/10.5167/uzh-65491>

Journal Article

Accepted Version

Originally published at:

Linden, Anthony; Llovera, Ligia; Herrera, Julio; Dorta, Reto; Agrifoglio, Giuseppe; Dorta, Romano (2012). “Chiral-at-Metal” Hemilabile Nickel complexes with a latent d10-ML2 Configuration: Receiving substrates with open arms. *Organometallics*, 31(17):6162–6171.

DOI: <https://doi.org/10.1021/om300484z>

‘Chiral-at-Metal’ Hemilabile Nickel Complexes with a Latent d^{10} -ML₂ Configuration: Receiving Substrates with Open Arms

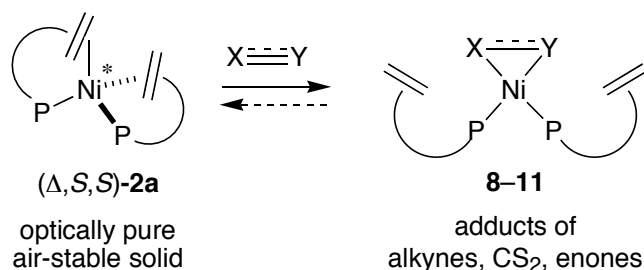
Anthony Linden,[‡] Ligia Llovera,⁺ Julio Herrera,[§] Reto Dorta,[#] Giuseppe Agrifoglio,[§] Romano Dorta^{§*}

[‡] *Organisch-Chemisches Institut, Universität Zürich, Winterthurerstr. 190, 8057 Zurich, Switzerland*

⁺ *Centro de Química, Instituto Venezolano de Investigaciones Científicas, Altos de Pipe, Venezuela*

[#] *School of Chemistry and Biochemistry, University of Western Australia, 35 Stirling Highway, Crawley 6009, Australia*

[§] *Departamento de Química, Universidad Simón Bolívar, Valle de Sartenejas, Caracas 1080A, Venezuela. E-mail: rdorta@usb.ve*



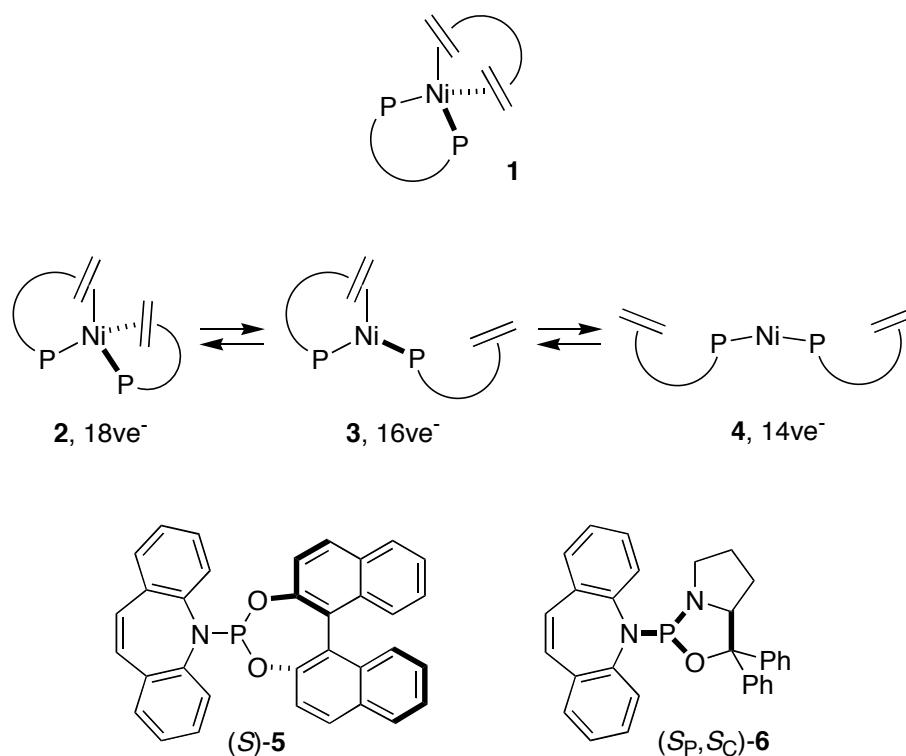
Abstract

Complexes with highly reactive stereogenic metal centers are of great interest to asymmetric synthesis. Thus, by reacting [Ni(COD)₂] with 2 equiv of the P,alkene ligands (*S*)-**5** ((*S*)-(+)-*N*-(3,5-dioxa-4-phosphacyclohepta[2,1-*a*;3,4-*a'*]dinaphthalen-4-yl)-dibenz[*b,f*]azepine) or (*S_P*,*S_C*)-**6** ((2*S*,5*S*)-(-)-*N*-(Aza-3-oxa-2-phosphabicyclo[3.3.0]octan-4-on-2-yl)-dibenz[*b,f*]azepine), the diastereomerically and enantiomerically pure tetrahedral complexes (Δ,*S*,*S*)-[Ni(**5**-κ*P*,η²-alkene)₂] (**2a**) and (Δ,*S_P*,*S_C*,*S_{P'}*,*S_{C'}*)-[Ni(**6**-κ*P*,η²-alkene)₂] (**2b**) were obtained in almost quantitative yields on multi-gram scales. The Ni atoms showed in both cases stable (Δ) configurations. Even though these Ni(0) complexes were air-stable in the solid state, once dissolved, complex **2a** readily activated CS₂, alkynes, and enones as the formal d^{10} -ML₂ fragment [Ni(**5**-κ*P*)₂] (**4**) to form adducts **8–11**. This is possible thanks to the decoordination of the hemilabile alkene arms of the P,alkene ligands, and the X-ray crystal structures of the CS₂ and 4-ethynyltoluene adducts confirmed the η² coordination modes of the substrates and the concomitant opening up of the alkene arms of ligand **5**. The coordination of α,β-unsaturated carbonyl compounds in complexes **11a–c** was reversible.

Introduction

Oxidative addition reactions to inherently unreactive closed shell tetrahedral d^{10} - ML_4 complexes only occur after ligand dissociation leads to unsaturated d^{10} - ML_2 or d^{10} - ML_3 species with 14 or 16 valence electrons (ve^-), respectively (see for instance the chemistry of the widely used catalyst precursor $[Pd(PPh_3)_4]$).¹ In the case of the common tetrahedral $[Ni(PP)(dialkene)]$ precursors of topology **1**² (see Scheme 1) usually the dialkene ligand (*e.g.* 1,5-cyclooctadiene, COD) dissociates irreversibly during reaction to liberate the reactive d^{10} - ML_2 fragment. However, it is often difficult to then stabilize such species towards decomposition.³ In fact, not many examples of isolable d^{10} - ML_2 complexes exist because they tend to be highly reactive and air-sensitive,⁴ and NiL_2 complexes are especially rare.^{4f} Hemilabile ligands⁵ such as the P,alkene phosphoramidites **5** and **6**⁶ with weakly coordinating alkene functions⁷ may mask such reactive Ni species by forming d^{10} - ML_4 complexes of type **2**⁸ which are connected to the latent d^{10} - ML_3 and d^{10} - ML_2 configurations **3**⁹ and **4** through successive hemilabile equilibria. In **4** the de-coordinated alkene functions nevertheless have a high effective concentration to stabilize the metal center. There is some evidence that ligands with secondary donor functions perform well in a variety of Ni-catalyzed asymmetric C-C bond forming reactions.¹⁰

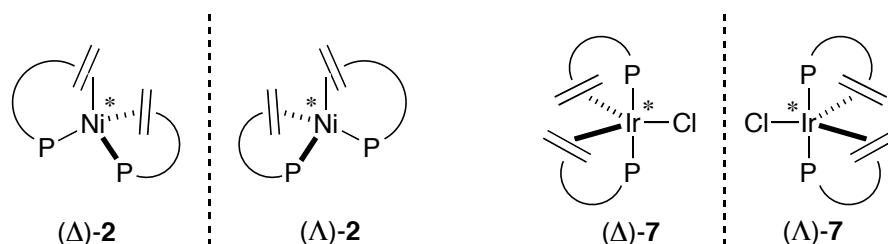
Scheme 1. Classic topology of **1** vs. topology of **2** attainable with P,alkene ligands **5** and **6** permitting hemilabile equilibria leading to d^{10} - ML_2 species **4**



Complexes of type **2** are also good candidates for the fixation and activation of small molecules. For example, L_2Ni-CO_2 complexes¹¹ are key intermediates in catalytic systems that use CO_2 as feedstock,¹² and even though analogous L_2Ni-CS_2 model complexes¹³ seem more amenable to isolation,¹⁴ a common feature of such activating $Ni(0)$ species is their pronounced air-sensitivity. We show in this paper that *air-stable* hemilabile $Ni(0)$ complexes of type **2**, once dissolved in the appropriate solvent, become highly reactive equivalents of $d^{10}-ML_2$ fragments which readily activate small molecules such as CS_2 , alkynes, and enones. In particular, we prove the hemilability of the P,alkene ligand system structurally: Single-crystal X-ray diffraction analyses reveal that both alkene arms of the ligands in type **2** complexes swing open to accommodate and activate the CS_2 ¹⁵ and ethynyltoluene molecules,¹⁶ thus demonstrating that a latent $d^{10}-ML_2$ species **4** is operational.

Most important from a stereochemical perspective is the fact that complexes of topology **2** possess stereogenic metal centers (“chiral-at-metal” complexes, see Scheme 2).¹⁷ Presently, the development of enantioselective catalysts is almost exclusively ligand-based, and an axiom of ligand design is to move stereogenic elements as close as possible to the metal center. Naturally then, complexes with stereogenic metals have been intensively studied, and the vast majority of them are pseudo-octahedral species stabilized by η^5-Cp^- or η^6 -arene type ligands^{17, 18} which were used in stereoselective stoichiometric¹⁹ and catalytic²⁰ transformations. So far, Noyori’s octahedral $[Ru(II)-BINAP-biscarboxylato]$ and $[Ru(II)-\eta^6$ -arene-*N*-tosylethylenediamine] complexes are the most compelling evidence for the effectiveness of stereogenic-at-metal complexes in asymmetric catalysis.²¹ Trigonal bipyramidal complexes of type **7** (Scheme 2) also present stereogenic metal centers, and, by using ligand **5**, we recently synthesized the diastereomerically and enantiomerically pure and configurationally stable Ir complex (Δ,S,S)-**7**.^{22a} Carreira and co-workers showed this complex to be a highly competent catalyst in enantioselective allylic etherifications^{22b} and aminations.^{22c} Tetrahedral optically pure stereogenic-at-metal complexes are rare,²³ and recently Schrock and Hoveyda described a series of remarkable tetrahedral complexes with stereogenic Mo and W atoms that are highly enantioselective ring-closing-metathesis catalysts.²⁴ Thus, we also show here that optically pure and configurationally stable tetrahedral $Ni(0)$ complexes of type **2** are easily accessible on gram scales by employing the phosphoramidite P-alkene ligands **5** and **6**.

Scheme 2. Stereogenic-at-metal complexes with phosphoramidite P,alkene ligands of type **5** and **6**



Experimental Section

General Considerations: All reactions were carried out under anaerobic and anhydrous conditions, using standard Schlenk and glove box techniques (MBraun Labmaster). THF, Et₂O, and benzene were distilled from deep purple Na/Ph₂CO solutions, toluene from Na, C₆D₆, THF-D₈ from Na₂K, and pentane and hexane from Na₂K/tetraglyme. CS₂, CH₃CN, CH₂Cl₂, and CD₂Cl₂ were degassed with three freeze-pump-thaw cycles and distilled from CaH₂. Only crystalline bright yellow [Ni(COD)₂] was used.²⁵

5 ((*S*)-(+)-*N*-(3,5-dioxa-4-phosphacyclohepta[2,1-*a*;3,4-*a'*]dinaphthalen-4-yl)-dibenz[*b,f*]azepine) and **6** ((2*S*,5*S*)-(-)-*N*-(Aza-3-oxa-2-phosphabicyclo[3.3.0]octan-4-on-2-yl)-dibenz[*b,f*]azepine) were prepared according published protocols.⁶ Diphenylacetylene (2.5 g) was recrystallized from dry boiling EtOH (11 mL) and thoroughly vacuum-dried. 4-Ethynyltoluene, 2-cyclohexenone, and 2-cyclopentenone (Aldrich) were purified by Kugelrohr distillation, degassed, and the enones were then kept over MS-4Å. Coumarine (Aldrich) was degassed. NMR spectra were recorded on Jeol 400 MHz and Bruker 500 MHz spectrometers. ATR-FTIR measurements were performed on a constant path transmission cell of ZnSe (Pike Technology) attached to a Bruker Tensor 27 spectrometer and samples were handled in air for brief periods of time. Elemental analyses were performed at IVIC or OCI and samples were handled in air.

(Δ,*S,S*)-[Ni(5**)₂] (**2a**):** A white slurry of (*S*)-**5**·0.05C₇H₈ (7011 mg, 13.69 mmol, as toluene solvate) in toluene (60 mL) was added over 10 min. to a vigorously stirred yellow solution of Ni(COD)₂ (1883 mg, 6.845 mmol) in toluene (40 mL) to afford a red clear solution. Stirring for 15 h afforded copious amounts of an orange microcrystalline precipitate. The mixture was concentrated to *ca.* half its initial volume, and pentane (100 mL) was added. The mixture was slurried for 3 h after which the solid was separated by filtration (GF/B glasfiber). The filter cake was thoroughly washed with hexanes (4 x 50 mL) and the yellow solid dried *in vacuo* (7.80 g, 96%). ³¹P{¹H} NMR (162 MHz, THF-D₈) δ 207.3 (s). ¹H NMR (400 MHz, THF-D₈) δ 5.05-5.25 (m, 4H), 5.55 (t, 2H), 5.98 (d, 2H), 6.70-6.90 (m, 4H), 6.90-

7.65 (m, 26H), 7.85 (d, 2H), 7.90-8.10 (m, 4H). The spectrum indicated the presence of 1.3 equiv of co-crystallized hexane. ^{13}C NMR (101 MHz, THF- D_8) δ 121.7, 123.8, 124.0, 124.4, 125.7, 126.0, 126.2, 126.5, 126.7, 126.8, 126.9, 127.9, 128.2, 128.4, 128.6, 129.1, 129.3, 129.6, 129.7, 129.8, 130.1, 132.5, 132.6, 132.7, 132.8, 133.7, 133.8, 141.8, 142.5, 143.0, 143.4, 149.7, 150.2. Depending on the quality of $\text{Ni}(\text{COD})_2$ re-crystallization was sometimes necessary to remove traces of metallic Ni: 2.90 g of the complex were dissolved in THF (100 mL) and filtered over a Celite-covered GF4 filter frit. The resulting bright orange solution was exposed to pentane vapor (100 mL) during 8 d to yield large orange crystals that were collected and dried *in vacuo* (2.25 g, 76%, ^1H NMR showed the presence of *ca.* 1.5 equiv of co-crystallized THF). Elemental analysis: C 74.97, H 4.50, N 2.40. Calculated for $\text{C}_{68}\text{H}_{44}\text{N}_2\text{NiO}_4\text{P}_2 \cdot 1.5\text{C}_4\text{H}_8\text{O}$: C 75.20, H 4.78, N 2.37. Single crystals of X-ray diffraction quality were obtained by exposing a solution of **2a** (50 mg) in THF- D_8 (0.6 mL) to *n*-pentane vapor.

(Δ,S,S,S,S)-[Ni(6**)₂] (**2b**):** A solution of (*R_p*,*S_C*)-**6** (1231 mg, 2.594 mmol) in benzene (5 g) was added dropwise over 5 min. to a vigorously stirred yellow slurry of $\text{Ni}(\text{COD})_2$ (356.9 mg, 1.297 mmol) in benzene (3 g) to afford a clear red solution. After stirring for 1 h the volatiles were evaporated *in vacuo* leaving an orange solid foam that was slurried and washed with pentane (3 x 20 mL, filtrations over glass fiber filter GF/B). The filter cake was dried in HV to yield 1.25 g (96%) of a bright yellow soft powder. Elemental analysis found: C 73.80, H 5.66, N 5.34. Calculated for $\text{C}_{62}\text{H}_{54}\text{P}_2\text{N}_4\text{NiO}_2$: C 73.89, H 5.40, N 5.56. $^{31}\text{P}\{^1\text{H}\}$ NMR (162 MHz, C_6D_6) δ 174.8 (s). ^1H NMR (400 MHz, C_6D_6) δ 0.90-1.05 (m, 2H), 1.15-1.30 (m, 2H), 1.35-1.50 (m, 2H), 1.50-1.65 (m, 2H), 2.20-2.35 (m, 2H), 3.45-3.60 (m, 2H), 4.55-4.70 (m, 2H), 5.00 (t, 2H), 5.50-5.65 (m, 2H), 6.30-6.40 (m, 2H), 6.70-7.55 (m, 34H). ^{13}C NMR (101 MHz, C_6D_6) δ 14.3, 22.7, 28.9, 34.4, 44.9, 45.1, 61.4, 69.2, 72.7, 73.0, 91.5, 91.7, 125.5, 125.7, 126.2, 126.5, 126.6, 126.9, 127.2, 129.5, 132.1, 143.0, 143.4 (br), 143.5 (br), 144.0, 146.4. Single crystals suitable for an X-ray diffraction analysis were obtained by dissolving 53 mg of **2b** in 5.3 g of boiling CH_3CN , filtering the hot solution through a cotton plug, and allowing the solution to cool slowly to RT by guarding it in a Dewar vessel. NMR spectra of these crystals corresponded to the product synthesized at RT.

(S,S)-[Ni(5**)₂(η^2 - CS_2)] (**8**):** CS_2 (104 mg, 1.37 mmol) in THF (6.0 g) was added dropwise over 15 min to a stirred orange-yellow slurry of **2a**·1.3 C_6H_{14} (1204 mg, 1.015 mmol, as hexane solvate) in THF (6.0 g) immediately affording a clear Bordeaux-red solution. After stirring for 0.5 h the solution was filtered over Celite and then pumped down to a glassy red solid and left under vacuum for 4 h. The solid was slurried and washed in Et_2O (2x20 mL), separated by filtration, and dried *in vacuo* (1081 mg, 91%, mustard yellow powder). ATR-FTIR: ν = 1183 cm^{-1} (s, C=S). $^{31}\text{P}\{^1\text{H}\}$ NMR (162 MHz, CD_2Cl_2): AB

quartet, δ 155.0 (apparent $J = 21$ Hz), 155.9 (apparent $J = 21$ Hz). ^1H NMR (400 MHz, CD_2Cl_2) δ 4.95-5.05 (m, 1H), 5.25-5.35 (m, 1H), 5.50-5.60 (m, 1H), 5.85-6.05 (m, 3H), 6.10-6.20 (m, 1H), 6.25-6.35 (m, 1H), 6.35-6.65 (m, 5H), 6.65-6.95 (m, 4H), 7.00-7.55 (m, 19H), 7.60-7.70 (m, 1H), 7.75-8.10 (m, 8H). The spectrum indicates the presence of *ca.* 0.25 equiv of Et_2O of co-crystallization. ^{13}C NMR (101 MHz, CD_2Cl_2) δ 120.8, 121.1, 122.3, 122.4, 122.6, 123.0, 124.8, 124.9, 125.2, 125.3, 125.6, 125.8, 125.9, 126.0, 126.2, 126.3, 126.5, 126.8, 126.9, 127.2, 127.3, 127.6, 127.7, 127.9, 128.1, 128.5, 128.6, 128.7, 128.9, 129.2, 129.4, 129.6, 129.7, 129.8, 129.9, 130.2, 130.5, 130.7, 130.8, 131.1, 131.8, 132.0, 132.1, 132.8, 133.1, 134.8, 135.1, 135.5, 135.7, 139.8, 140.0, 140.7, 140.9, 147.7, 148.6, 148.7, 149.0, 149.1, 149.2, 255.3 (d, $J_{\text{PC}} = 67.2$ Hz). Crystalline material was obtained as follows: Pentane (8 mL) was added dropwise to a stirred, filtered solution of 0.50 g of **8**·0.25 Et_2O in 11.5 g CH_2Cl_2 (limit of solubility), and the resulting slightly turbid dark red solution was left undisturbed for 2 h at RT (**8** is not stable in CH_2Cl_2 solution over extended periods of time). The microcrystalline solid was collected and dried in the glovebox atmosphere (0.33 g, 63%, NMR data correspond and indicate the presence of *ca.* 0.8 equiv of CH_2Cl_2 of co-crystallization). Single crystals suitable for an X-ray diffraction analysis were obtained by layering a solution of **8** (40 mg) in CD_2Cl_2 (0.6 mL) with pentane (2 mL) in an NMR tube. Elemental analysis of the crystals found: C 70.09, H 3.95, N 2.32, S 4.83. Calculated for $\text{C}_{69}\text{H}_{44}\text{N}_2\text{NiO}_4\text{P}_2\text{S}_2\cdot 0.5\text{CD}_2\text{Cl}_2$: C 69.95, H 3.89, N 2.34, S 5.37.

(*S,S*)-[Ni(5**)₂(η^2 -PhCCPh)] (**9**):** A solution of diphenylacetylene (117 mg, 0.656 mmol) in toluene (2.3 g) was added dropwise to a vigorously stirred pre-cooled (250 K) orange slurry of **2a**·1.3 C_6H_{14} (519 mg, 0.438 mmol, as hexane solvate) in toluene (4.6 g). Within 5 min the slurry dissolved to give a clear orange solution that turned yellow within 10 min. After stirring for 1 h the solution was filtered over a Celite-covered cotton plug and evaporated to dryness. Slurrying in a Et_2O (6 mL)/pentane (6 mL) mixture afforded a lemon yellow microcrystalline solid that was separated by filtration and dried in HV (410 mg, 75 %, pale yellow powder). Elemental analysis found: C 77.90, H 4.46, N 2.23. Calculated for $\text{C}_{82}\text{H}_{54}\text{N}_2\text{NiO}_4\text{P}_2\cdot 0.6\text{Et}_2\text{O}$: C 78.19, H 4.66, N 2.16. The ^1H NMR spectrum shows the presence of two isomers (*ca.* 9:1) and *ca.* 0.6 equiv of Et_2O of co-crystallization. FTIR (Fluorolube): 1802 cm^{-1} (m, $\text{C}\equiv\text{C}$). $^{31}\text{P}\{^1\text{H}\}$ NMR (202 MHz, C_6D_6) δ 163.4 (s, 87% by integration), 165.2 (s, 13% by integration).

(*S,S*)-[Ni(5**)₂(η^2 -4-ethynyltoluene)] (**10**):** 4-Ethynyltoluene (130 mg, 1.12 mmol) was added dropwise to a vigorously stirred orange-yellow toluene (3.8 g) slurry of **2a**·1.3 C_6H_{14} (1108 mg, 0.9344 mmol, as hexane solvate) over 5 min. This immediately afforded a clear pale yellow solution that gradually turned brown-red over 20 min. After stirring for 2 h the solution was filtered over a Celite-covered cotton plug and then evaporated to a beige solid. Et_2O (9 mL) and pentane (9 mL) were added and the

microcrystalline product was slurried for 10h and cooled to 245 K to complete precipitation. The precipitate was separated by filtration and dried *in vacuo* (1045 mg, 94%, pale yellow soft powder). Elemental analysis found: C 76.52, H 4.32, N 2.35. Calculated for $C_{77}H_{52}N_2O_4P_2Ni \cdot 0.1C_7H_8$: C 77.83, H 4.44, N 2.34.²⁶ ATR-FTIR: $\nu = 1735\text{ cm}^{-1}$ (w, C \equiv C). $^{31}P\{^1H\}$ NMR (202 MHz, C_6D_6): AB quartet, δ 163.0 (apparent $J = 14.2$ Hz), 165.5 (apparent $J = 14.2$ Hz). 1H NMR (500 MHz, C_6D_6) δ 2.25 (s, 3H), 5.27 (m, 1H), 5.45 (m, 1H), 5.64 (m, 1H), 5.90 (m, 1H), 6.01 (m, 1H), 6.15-6.30 (m, 5H), 6.45 (m, 1H), 6.50-6.70 (m, 5H), 6.90-7.05 (m, 5H), 7.10 (m, 1H), 7.15-7.35 (m, 7H), 7.40-7.55 (m, 13H), 7.60-7.70 (m, 4H), 7.80 (m, 1H), 8.40 (m, 2H). The spectrum indicates the presence of *ca.* 0.1 equiv of toluene of co-crystallization. ^{13}C NMR (127 MHz, C_6D_6) δ 21.4, 121.6, 122.0, 122.4, 122.6, 123.3, 123.4, 123.6, 123.8, 124.7, 124.9, 125.5, 125.6, 125.9, 126.0, 126.2, 127.4, 127.5, 127.6, 128.5, 128.6, 128.7, 128.8, 128.9, 129.1, 129.3, 129.4, 129.5, 129.6, 129.9, 130.1, 130.2, 130.5, 130.7, 130.9, 131.0, 132.1, 132.2, 132.4, 132.5, 132.9, 133.0, 133.4, 133.8, 135.8, 135.9, 136.1, 136.4, 136.8, 142.1, 142.3, 142.4, 142.5, 143.0, 149.3, 149.8, 150.5, 150.6, 151.0, 151.1. Single crystals suitable for an X-ray diffraction analysis were grown from a C_6D_6 (0.6 mL) solution of **10** (50 mg) that was layered with Et_2O (1.2 mL) in an NMR tube.

Representative reaction of **2a with coumarine (**11c**):** A solution of coumarine (27.7 mg, 0.190 mmol) in THF (0.7 g) was added dropwise to a stirred orange slurry of **2a**· $1.3C_6H_{14}$ (102 mg, 0.0858 mmol, as hexane solvate) in THF (0.5 g). The resulting lemon yellow clear solution was stirred for 2h and then submitted to $^{31}P\{^1H\}$ NMR (202 MHz, C_6D_6) analysis: main AB quartet, δ 155.0 (apparent $J = 32$ Hz), 157.8 (apparent $J = 32$ Hz), 84% of all integrals; minor AB quartet, δ 157.6 (apparent $J = 29$ Hz), 158.1 (apparent $J = 29$ Hz), 11% of all integrals; minor AB quartet, δ 156.3 (apparent $J = 56$ Hz), 160.7 (apparent $J = 56$ Hz), 5% of all integrals. 1H NMR (500 MHz, C_6D_6) δ 3.90 and 4.21 (s, br, 2H, α,β -protons of coordinated coumarine), integral over the rest of signals (4.5–10.0 ppm) corresponded to *ca.* 54H (*i.e.* 48H of **11c**, 6H of 1 equiv of excess coumarine). Isolation: The volatiles of the solution were evaporated and the pale yellow solid slurried and washed in pentane (2x5 mL), filtered, and dried *in vacuo* (94 mg). The $^{31}P\{^1H\}$ NMR (202 MHz, C_6D_6) spectrum was identical to the above plus a new resonance at δ 209.6 (s, *ca.* 15% by integration), corresponding to complex **2a**.

X-ray crystal structure determinations: All measurements were carried out at 160 K on an Agilent Technologies SuperNova CCD diffractometer (Mo $K\alpha$ radiation, $\lambda = 0.71073\text{ \AA}$). Table 2 lists the pertinent crystal data. The intensities were corrected for Lorentz and polarization effects, and an absorption correction based on the multi-scan method²⁷ was applied. The structures were solved by direct methods using SHELXS97,²⁸ which revealed the positions of all non-H-atoms. The non-H-atoms

were refined anisotropically. All of the H-atoms were placed in geometrically calculated positions and refined by using a riding model where each H-atom was assigned a fixed isotropic displacement parameter with a value equal to $1.2U_{eq}$ of its parent C-atom ($1.5U_{eq}$ for any solvent methyl groups). The refinement of each structure was carried out on F^2 using the full-matrix least-squares procedures of SHELXL97, which minimized the function $\sum w(F_o^2 - F_c^2)^2$. The absolute structures, and hence the absolute stereochemistries of the molecules, have been determined by refinement of the absolute structure parameters (Table 1) according to the method of Flack and Bernardinelli.²⁹ For **2a**, the asymmetric unit contains one molecule of the Ni-complex plus two disordered THF molecules. One of the THF molecules could be seen in difference electron density peaks, but refinement yielded large atomic displacement parameters, indicating disorder or partial occupation of the site. The second THF molecule was not readily discernable from the difference electron density peaks. Therefore the *SQUEEZE* routine³⁰ of the program *PLATON*³¹ was employed. When the solvent molecules are omitted from the model, each unit cell contains three cavities of 2073 \AA^3 located on three-fold axes. The electron count in each cavity was calculated to be approximately $217 e^-$, which corresponds with approximately six molecules of THF ($240 e^-$). This assumption was used in the subsequent calculation of the empirical formula, formula weight, density, linear absorption coefficient and $F(000)$. Based on the assumption, the ratio of Ni-complex to THF molecules in the structure is 1:2. For **2b**, the asymmetric unit contains three molecules of the Ni-complex and four disordered molecules of MeCN. Two sets of overlapping positions were defined for the atoms of two of the MeCN molecules and the site occupation factors of the major conformations of these molecules refined to 0.613(18) and 0.68(3). Similarity restraints were applied to the chemically equivalent bond lengths and angles involving all disordered atoms, while neighbouring atoms within and between each orientation of the disordered molecules were restrained to have similar atomic displacement parameters. For **8**, the asymmetric unit contains one molecule of the Ni-complex plus one molecule of CD_2Cl_2 . For **10**, the asymmetric unit contains one molecule of the Ni-complex plus one disordered Et_2O molecule and one C_6D_6 molecule. The C_6D_6 molecule could not be modelled adequately, so the *SQUEEZE* routine was again employed in a similar way to that described for **2a**. Each unit cell contains two cavities of 565 \AA^3 with a calculated electron count of approximately $70 e^-$ per cavity, which is a little less than two molecules of C_6D_6 ($42 e^-$) per cavity. It is therefore assumed there is one molecule of C_6D_6 per asymmetric unit and thus the ratio of Ni-complex molecules to Et_2O and C_6D_6 molecules in the structure is 1:1:1. The alkyne ligand is disordered over two conformations which was modeled in a similar way to that described for **2b**. The site occupation factor of the major conformation of this ligand refined to 0.572(10).

Table 1. Crystal data and refinement parameters of compounds **2a**, **2b**, **8**, and **10**^a

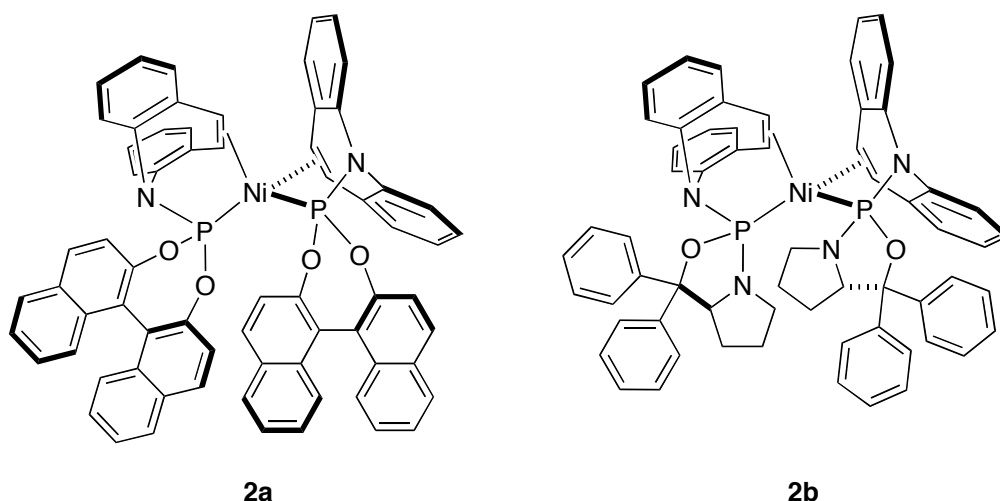
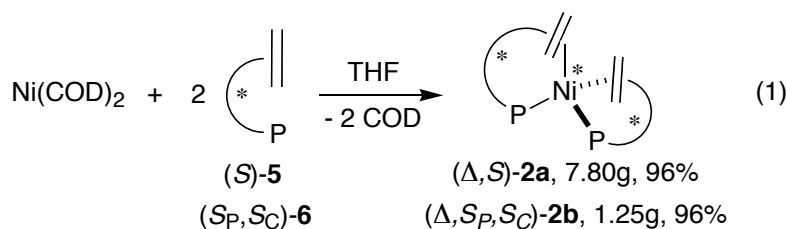
	2a ·2THF·D ₈	2b ·1.33CH ₃ CN	8 ·CD ₂ Cl ₂	10 ·Et ₂ O·C ₆ D ₆
formula	C ₇₆ H ₄₄ D ₁₆ N ₂ NiO ₆ P ₂	C _{64.67} H _{58.1} N _{5.33} NiO ₂ P ₂	C ₇₀ H ₄₄ Cl ₂ D ₂ N ₂ NiO ₄ P ₂ S ₂	C ₈₇ H ₆₂ D ₆ N ₂ NiO ₅ P ₂
<i>M</i> (g mol ⁻¹)	1234.08	1062.52	1236.84	1348.19
crystal system	trigonal	monoclinic	orthorhombic	orthorhombic
space group	<i>R</i> 3	<i>P</i> 2 ₁	<i>P</i> 2 ₁ 2 ₁ 2 ₁	<i>P</i> 2 ₁ 2 ₁ 2 ₁
<i>a</i> (Å)	37.5195(6)	11.73863(10)	12.4492(2)	12.5470(3)
<i>b</i> (Å)	37.5195(6)	11.70932(11)	14.1316(2)	22.4042(5)
<i>c</i> (Å)	13.4940(2)	58.7106(5)	32.7302(5)	25.2593(6)
β (°)	90	92.4392(9)	90	90
<i>V</i> (Å ³)	16450.7(4)	8062.54(12)	5758.1(1)	7100.5(3)
<i>Z</i>	9	6	4	4
μ (mm ⁻¹)	0.358	0.472	0.612	0.374
<i>D_c</i> (g cm ⁻³)	1.106	1.313	1.424	1.255
2 θ_{max} (deg)	55.4	55.0	55.0	54.8
<i>T</i> (K)	160	160	160	160
reflns collected	56708	81234	44842	39344
indep refln, <i>R</i> _{int}	15371, 0.047	33051, 0.038	11952, 0.030	14458, 0.057
refln with <i>I</i> > 2 σ (<i>I</i>)	14304	31815	10627	11500
parameters refined	695	2089	749	906
GOF	1.065	1.198	1.029	1.046
<i>R</i> (<i>F</i>) [<i>I</i> > 2 σ (<i>I</i>) reflns]	0.0359	0.0593	0.0370	0.0548
<i>wR</i> (<i>F</i> ²) (all data)	0.1059	0.1199	0.0888	0.1505
$\Delta\rho$ (max; min) [e Å ⁻³]	0.35; -0.28	0.65; -0.78	0.71; -0.44	1.16; -0.35
absolute structure parameter	0.018(6)	0.034(8)	-0.012(9)	-0.02(1)

^a) Details of the treatment of solvent molecules and disordered ligands are in the experimental part and the deposited CIFs.

Results and discussion

Complexes with stereogenic Ni centers: The chiral Ni(0) complexes **2a** and **2b** were prepared by reacting 2 equiv of (*S*)-**5** and (*R_p*, *S_C*)-**6** (see Scheme 1)⁶ respectively, with [Ni(COD)₂] (COD = 1,5-cyclooctadiene) in toluene solution according to eq 1. These reactions were clean and quantitative on an NMR basis, and the bright orange analytically pure micro-crystalline products were reproducibly isolated in excellent yields on multi-gram scales. Recrystallization after filtration over Celite sometimes was necessary in order to eliminate small amounts of metallic Ni dragged along from the [Ni(COD)₂] starting material. Complexes **2a** and **2b** in the solid state are stable in moist air for several

days. The solubility of crystalline **2a** is low in aromatics, medium in THF, and high in chlorinated solvents, whereas crystalline **2b** is generally much more soluble. Orange CD₂Cl₂ and CDCl₃ solutions of both complexes decomposed within minutes to afford greenish mixtures, presumably *via* C-Cl activation of the chlorinated solvents.³²



The $^{31}\text{P}\{^1\text{H}\}$ NMR spectra of **2a** and **2b** displayed sharp singlets at δ 209 and 175, respectively. [^1H , ^{31}P] and [^1H , ^{13}C] HMQC NMR experiments in C_6D_6 solution identified the ^1H and ^{13}C signals of the coordinated alkene functions: In **2a** the protons resonate at δ 5.14 (d, 2H) and 5.40 (m, 2H), and the carbon nuclei at δ 71.3 and 69.5, while in **2b** the protons resonate at δ 4.46 (m, 2H) and 5.58 (m, 2H) and the carbon nuclei at δ 72.9 and 61.4. Variable temperature $^{31}\text{P}\{^1\text{H}\}$ NMR studies between $-80\text{ }^\circ\text{C}$ and $+80\text{ }^\circ\text{C}$ in toluene solution were undertaken in order to probe the configurational stability of the Ni centers in **2a** and **2b**.³³ Apart from small variations in linewidths and chemical shifts ($\Delta\delta < 2\text{ ppm}$), no new resonances appeared in the aforementioned temperature window. These observations suggest *perfect diastereoselectivities* of the complexation reactions with respect to Ni stereochemistry and configurational stability of the complexes.

In order to elucidate the precise molecular structures and the absolute configurations of the Ni centers, single crystals of **2a** and **2b** were grown from THF/*n*-pentane and CH₃CN solutions, respectively, and

subjected to X-ray diffraction analyses. As expected, complexes **2a** and **2b**, as their respective THF and CH₃CN solvates, are monomeric and display tetrahedral coordination spheres around the Ni atoms (see Figures 1 and 2 and Table 1 for the crystal data and refinement parameters of all reported crystal structures) thanks to a bidentate coordination mode of the P,alkene ligands. Complex **2a** shows a pseudo *C*₂ point symmetry which is evidenced in the inset of Figure 1. It is noteworthy that the asymmetric unit of **2b** contains three independent molecules of the Ni-complex and four disordered molecules of CH₃CN. Both complexes in their respective crystals are enantio- and diastereomerically pure and the absolute configurations of the molecules have been determined independently by the diffraction experiment. In order to exclude the possibility of epimerization of the metal stereocenter or the stereogenic P atoms in **2b** during crystallization from boiling CH₃CN to obtain the X-ray quality single crystals (see experimental part), a separate ³¹P and ¹H NMR analysis of a C₆D₆ solution of such crystals established their identity with **2b** from bulk preparations. The data confirmed the identity with bulk preparations and the configurational stability of **2b** in hot CH₃CN. In both cases the optically pure modifiers used in the ligand syntheses ((*S*)-binaphthol and (*S*)-diphenylprolinol) showed the expected configurations. Most importantly, these structures allowed us to assign the absolute configurations of the Ni stereocenters, which are (Δ) in both cases.

As observed in other complexes and in the free ligands **5** and **6**,^{6, 7a, 22a} the benzazepine moiety adopts a boat conformation that allows for an effective bidentate metal complexation. The average bite angle spanned by the mid-points of the alkenes, the Ni centres, and the P atoms is 93.8(1)° in **2a** and 95.13(3)° in **2b**, thanks in both cases to a distinctly pyramidal (*i.e.* *sp*³) geometry of the benzazepine-N atoms: The sum of the bond angles at N1 and N2 in complex **2a** are 335.9(2)° and 334.3(3)°, respectively, and in complex **2b** they range from 335.9(5) to 337.6(5)° across the three independent molecules. Note that in the free ligands **5**⁶ and **6**³⁴ this same N atom was shown to be perfectly trigonal planar. The mean Ni–P and Ni–C distances for **2a** are 2.1249(7) Å and 2.097(8) Å, respectively, and for all independent molecules of **2b** they are 2.141(2) and 2.09(1) Å, respectively. In Bennett's triarylphosphine-based [Ni(P,alkene)₂] complex⁸ the corresponding Ni–P bonds are longer (2.19–2.20 Å), while the corresponding Ni–C are slightly shorter (mean value of 2.04 Å). Both observations are consistent with a lower electron density on Ni in our complexes due to the higher π-acidity of the phosphoramidite P atoms. The alkene bonds in the free ligands **5** and **6** measure 1.34 Å⁶ and 1.33 Å,³⁴ and upon coordination to the Ni centers in complexes **2a** and **2b** they elongate to an average of 1.405(4) and 1.41(2) Å, respectively. These distances are in good agreement with values found in

electron rich Ni(0) complexes,^{2b,d, 8} even though phosphoramidite ligands are expected to lead to electron poorer metal centers when compared to phosphines.

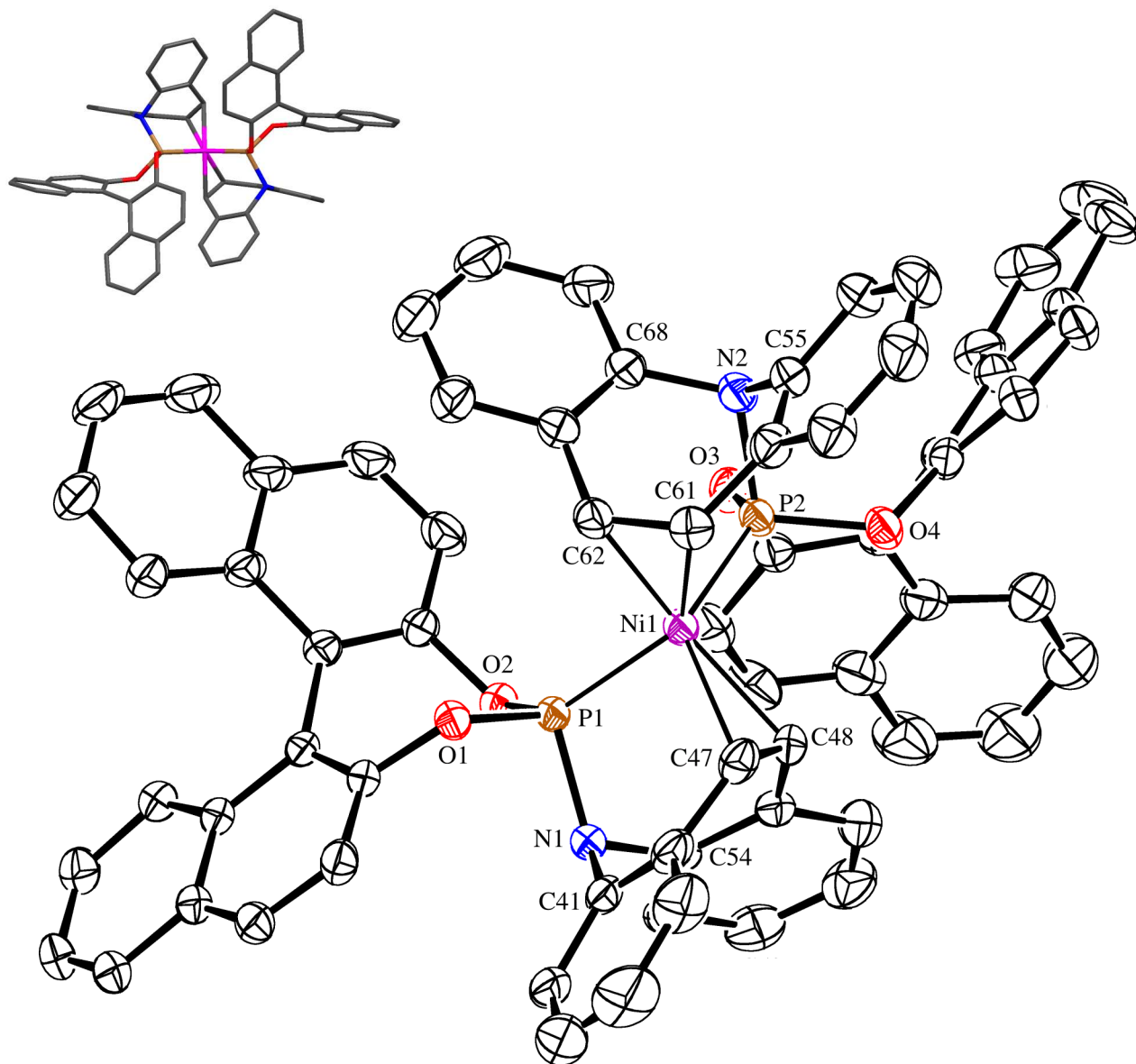


Figure 1. The molecular structure of complex (Δ, S_a, S_a)-2a in the crystal (50% probability ellipsoids, hydrogen atoms are omitted). The inset is a view along the C₂-axis of the complex. Selected bond lengths (Å) and angles (deg) are: Ni1–P1, 2.1270(5); Ni1–P2, 2.1228(5); Ni1–C47, 2.111(2); Ni1–C48, 2.072(2); Ni1–C61, 2.110(2); Ni1–C62, 2.081(2); P1–N1, 1.714(2); P1–O1, 1.625(1); P1–O2, 1.642(1); P2–N2, 1.724(2); P2–O3, 1.641(2); P2–O4, 1.629(1); C47–C48, 1.406(3); C61–C62, 1.403(3); P1–Ni1–P2, 118.85(2); Ni1–P1–N1, 109.65(6); Ni1–P2–N2, 109.70(7); P1–N1–C41, 113.3(1); P2–N2–C55, 111.9(1). Torsion angles ϕ along the P–N vectors (see text for the definition and Scheme 4): 6.1 (P1–N1), 4.9 (P2–N2).

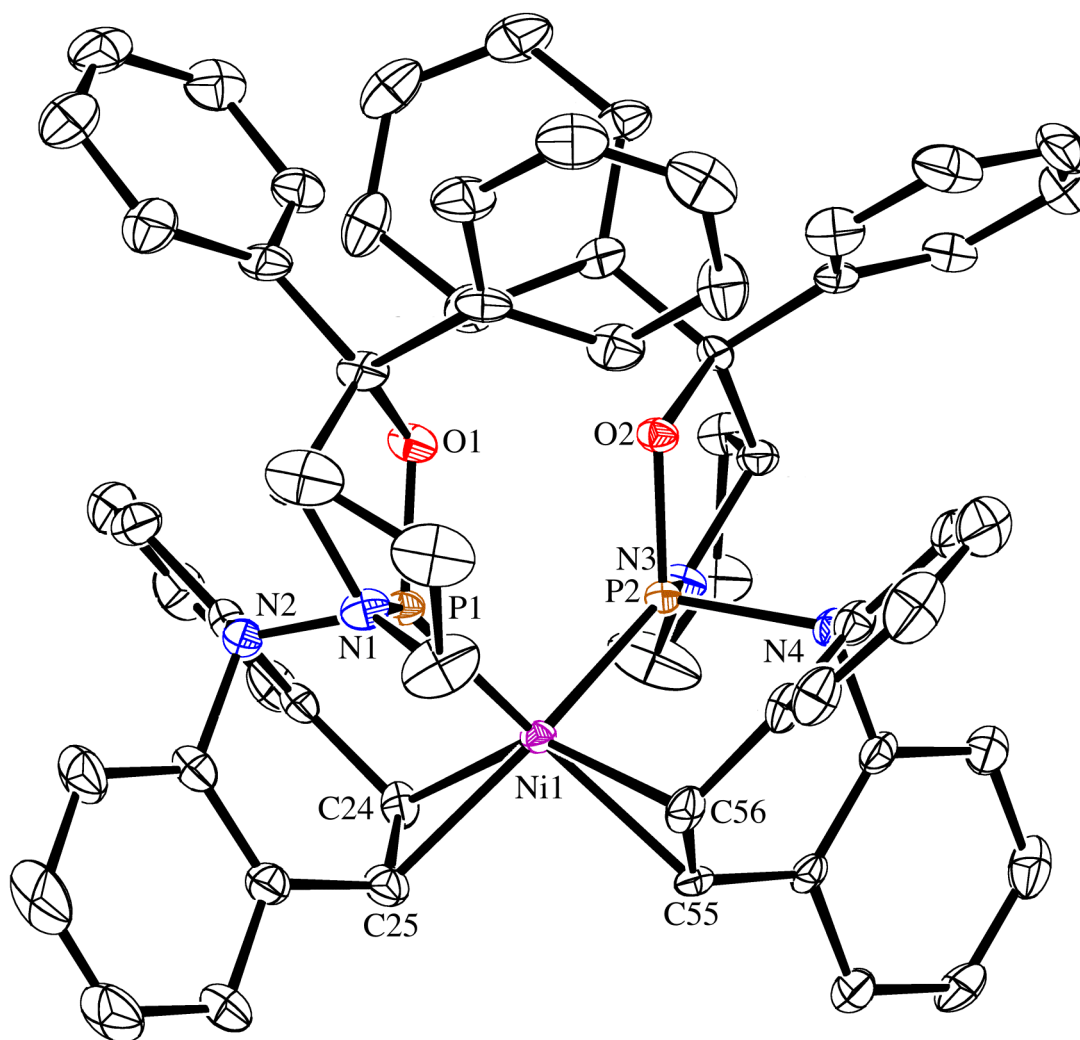


Figure 2. The structure of one of three independent molecules of the complex $(\Delta,R_p,R_{p'},S_C,S_{C'})$ -**2b** in the crystal (50% probability ellipsoids, hydrogen atoms are omitted). Selected bond lengths (Å) and angles (deg) are: Ni1-P1, 2.154(1); Ni1-P2 2.132(1); Ni1-C24, 2.075(4); Ni1-C25, 2.108(4); Ni1-C55, 2.098(4); Ni1-C56, 2.081(4); P1-O1, 1.627(3); P1-N1, 1.665(3); P1-N2, 1.741(4); P2-O2, 1.616(3); P2-N3, 1.645(3); P2-N4, 1.758(3); C24-C25, 1.424(6); C55-C56, 1.421(6); P2-Ni1-P1, 103.36(4); C24-Ni1-P1, 98.4(1); C25-Ni1-P1, 92.0(1); C55-Ni1-P2, 91.9(1); C56-Ni1-P2, 97.5(1); C24-Ni1-C55, 106.8(2). Torsion angles ϕ along the P-N vectors (see text and Scheme 4 for the definition). Molecule A: 8.3 (P1-N2), 6.9 (P2-N4); Molecule B: 3.1 and 2.7; Molecule C: 7.8 and 10.6.

Activation of CS₂, alkynes, and enones: In view of potential applications in asymmetric synthesis, we were interested to assess the reactivity of complex **2a** towards promising substrates, such as CO₂ and its analogues, alkynes, alkenes, ketones, and enones. While **2a** did not react with CO₂ (1 bar),

dicylohexylcarbodiimide, or 1-naphthylisocyanate, a slight excess of CS₂ reacted quantitatively and in the time of mixing with a yellow slurry of complex **2a** in THF to afford a clear Bordeaux red solution (see Scheme 3). Compound **8** was isolated in excellent yield on a gram scale, and an ATR-FTIR spectrum was consistent with a η^2 coordinated CS₂ molecule showing a strong band at 1183 cm⁻¹ (see Figure 3). The ³¹P{¹H} NMR spectrum indicated desymmetrization of the molecule, showing an AB quartet centered around δ 155 and 156 (apparent $J = 21$ Hz), and the ¹³C{¹H} NMR spectrum showed a characteristic doublet at δ 255.3 ($J_{PC} = 67.2$ Hz, J_{PC} not resolved) which is in line with reported values.^{14c} The CS₂ coordination is irreversible, resisting vacuum (10⁻³ mmHg), recrystallizations, and washing with alkanes or ether.

The single crystal X-ray diffraction analysis of complex **8**, as its **8**·CD₂Cl₂ solvate, revealed the mononuclear structure depicted in Figure 4 and confirmed η^2 coordination of CS₂ with concomitant de-coordination of the ligand alkene functions. To the best of our knowledge, this represents the first example of a structurally authenticated chiral CS₂ metal complex.³⁵ As expected for a diamagnetic Ni(II) complex, the sulfa-nickela-cyclapropane ring is coplanar with the plane spanned by P1, P2, and Ni. The maximum deviation of atoms Ni1, S1, S2, C69, P1 and P2 from their mean plane is 0.029(1) Å for atom S2. The C69–S1 distance of 1.578(3) Å is the expected value for a C=S bond, and the η^2 coordinated portion C69–S2 of the CS₂ molecule is elongated to 1.685(3) Å. Expectedly, this distance is shorter in our phosphoramidite-ligated complex than in Hillhouse's trialkylphosphine-ligated [(dtbpe)Ni(η^2 -CS₂)] (dtbpe = 1,2-bis(di-*t*-butylphosphino)ethane) complex, where the corresponding distance of 1.732(6) Å^{14c} suggests a higher electron density at the Ni center and therefore stronger backbonding to the coordinated CS₂ molecule. In Mealli's pentacoordinate [(MeC(CH₂PPh₂)₃)Ni(η^2 -CS₂)] complex, by contrast, this bond is significantly shorter (1.63(1) Å).^{14b}

The opening up of the ligand alkene arms by going from the starting complex **2a** to complex **8** causes a geometry change of the N1 and N2 atoms from significantly pyramidal in **2a** to trigonal planar in **8** (see Scheme 4). The sum of the angles at both N1 and N2 is 360.0(3)°. The mean P–N distance in **8** is 1.663(3) Å, while in **2a** it is 1.719(2) suggesting that the N lone pair is involved in the P–N bond, giving it some double-bond character when the alkene arm is not coordinating. The mean C=C distance in the now uncoordinated alkenes of **8** is 1.327(5) Å, which corresponds to the bond lengths in the free ligands **5** and **6**, mentioned above.

Scheme 3

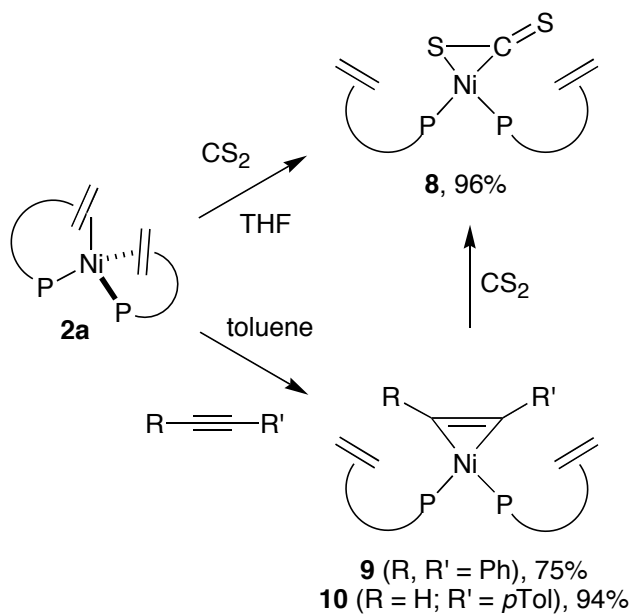
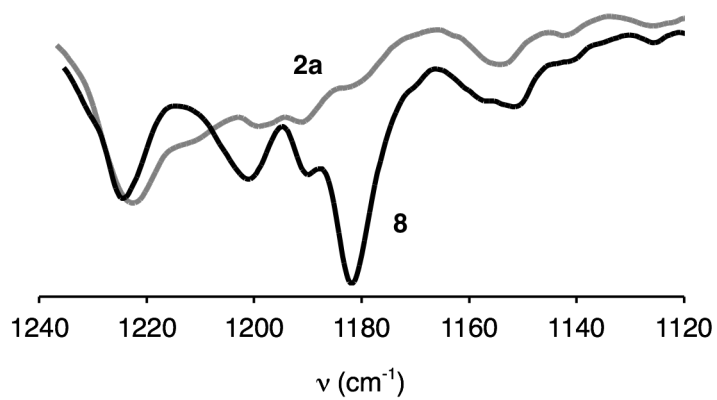


Figure 3. ATR-FTIR spectra of complexes **2a** (grey trace) and **8** (black trace)



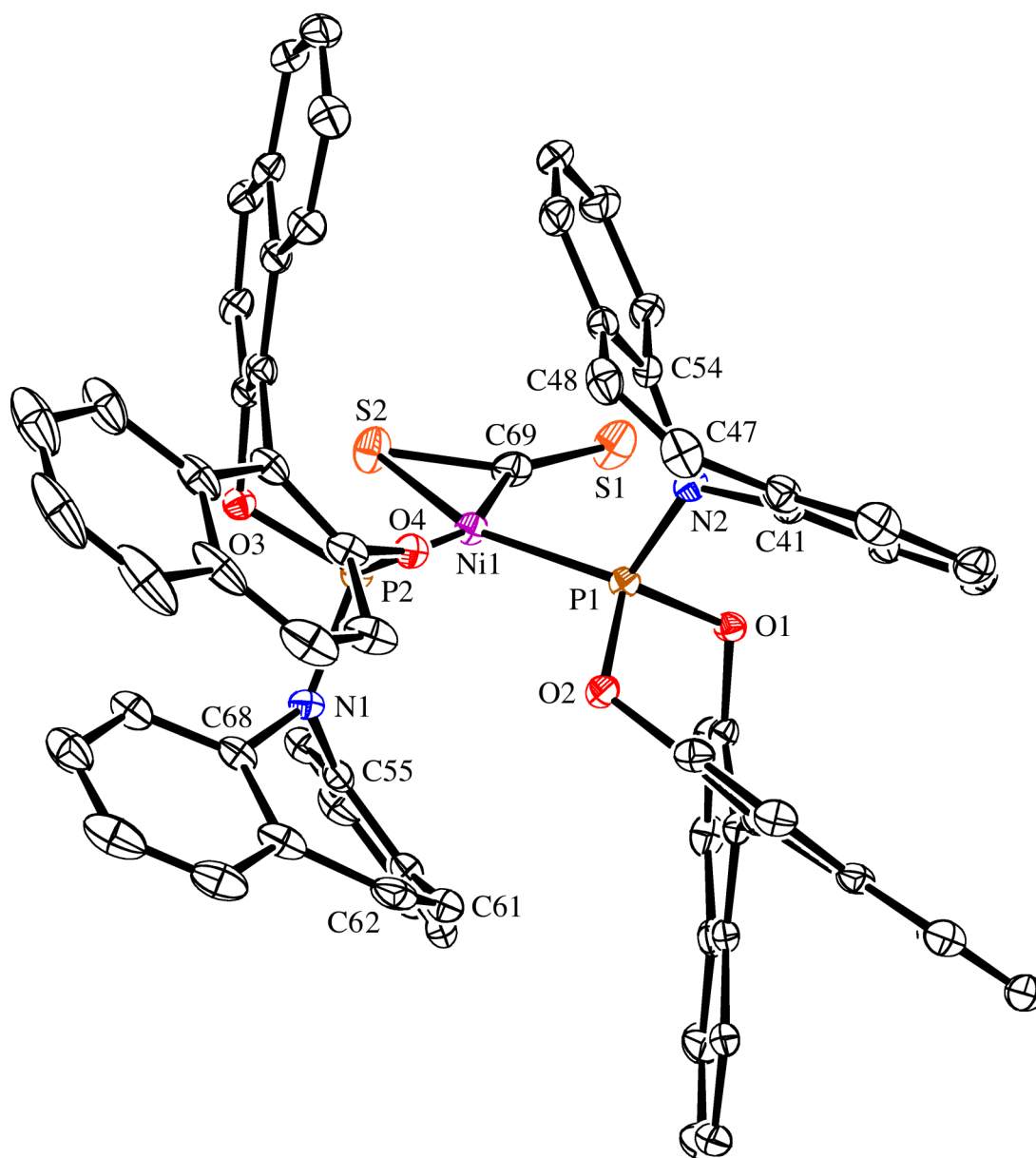


Figure 4. The molecular structure of complex (*S,S*)-**8** in the crystal (30% probability ellipsoids, hydrogen atoms are omitted). Selected bond lengths (Å) and angles (deg) are: Ni1–P1, 2.1195(7); Ni1–P2, 2.1879(7); Ni1–S2, 2.1529(8); Ni1–C69, 1.913(3); S1–C69, 1.587(3); S2–C69, 1.685(3); P1–N2, 1.664(2); P1–O1, 1.628(2); P1–O2, 1.620(2); P2–N1, 1.661(2); P2–O3, 1.632(2); P2–O4, 1.622(2); C61–C62, 1.327(4); C47–C48, 1.334(5); P1–Ni1–P2, 99.02(3); P1–Ni1–S2, 153.44(3); P1–Ni1–C69, 105.01(9); P2–Ni1–S2, 107.45(3); P2–Ni1–C69, 155.97(9); S2–Ni1–C69, 48.53(9); Ni1–S2–C69, 58.3(1); Ni1–C69–S2, 73.2(1); S1–C69–S2, 142.6(2); Ni1–C69–S1, 144.2(2); Ni1–P1–N2, 115.12(8); Ni1–P2–N1, 116.47(8); P1–N2–C41, 124.4(2); P2–N1–C55, 117.3(2). Torsion angles ϕ (see text for the definition and Scheme 4) along the P–N vectors: 79.2 (P1–N2), 81.9 (P2–N1).

While **2a** did not react with styrene or 1-hexene, the addition of 1.5 equiv of diphenylacetylene to an orange benzene slurry of **2a** led to a pale yellow solution, and product **9** (see Scheme 3) was isolated in good yield as a pale yellow microcrystalline solid. The $^{31}\text{P}\{^1\text{H}\}$ NMR spectrum showed a major (87% of integrals) singlet at δ 163.4 consistent with a C_2 -symmetric adduct. On the other hand, 1.2 equiv of 4-ethynyltoluene reacted with an orange slurry of **2a** to afford a clear pale yellow solution of **10**, but this time its $^{31}\text{P}\{^1\text{H}\}$ NMR spectrum showed an AB quartet centered at δ 163.0 and 165.5 with an apparent $J = 14.2$ Hz, as would be expected for an adduct of lower symmetry. The resonance of the acetylenic H is shifted strongly downfield to δ 7.67 when compared to free 4-ethynyltoluene (δ 3.05) displaying an ABX quartet by coupling to the P atoms ($J_{\text{HP}} = 42.8$ Hz, $J_{\text{HP}'} = 15.9$ Hz). **10** was isolated in excellent yield on a gram scale as a pale yellow powder. The addition of slight excesses of CS_2 to pale yellow slurries of the alkyne complexes **9** and **10** in C_6D_6 afforded deep red clear solutions in the time of mixing. $^{31}\text{P}\{^1\text{H}\}$ NMR analyses showed quantitative formation of the CS_2 adduct **8** in both cases (Scheme 3).

Single crystals of adequate quality grew as the $\text{10} \cdot \text{C}_6\text{D}_6 \cdot \text{Et}_2\text{O}$ solvate from a $\text{C}_6\text{D}_6/\text{Et}_2\text{O}$ mixture, and the X-ray diffraction analysis confirmed the expected η^2 coordination of the alkyne function and the de-coordinated, open alkene arms of the ligands in the mononuclear, distorted square planar Ni(II) complex (Figure 5).³⁶ We note that structurally characterized complexes of H-substituted alkynes are quite rare,³⁷ and that in catalytic systems such species are thought to undergo oxidative addition of the acetylenic C-H bond to form $\text{Ni}^{\text{II}}(\text{H})(\text{alkynyl})$ intermediates.³⁸ Even heating a benzene solution of complex **10** to 70° C for 30 minutes did not cause any reaction; in particular no hydrides product of C-H activation were observed. The 4-ethynyltoluene ligand in **10** is disordered over two conformations that are nearly overlapping. The molecular structure of **10** is extremely similar to that of **8**, as shown by the overlay in Figure 6. However, the nickela-cyclapropane ring is slightly tilted with respect to the plane spanned by P1, P2, and Ni giving a dihedral angle of 11.9(13)° for the major conformation of the ligand and 7.8(17)° for the minor conformation. The distance of the coordinated alkyne function C69–C70 of 1.265(7) Å is only *ca.* 0.01 Å shorter than in comparable electron rich diphosphine stabilized Ni complexes.^{36c,h,n, 37b} Corresponding complexes stabilized by phosphite ligands are scarce,^{36 k} and we are unaware of structurally characterized η^2 -alkyne Ni adducts bearing phosphoramidite ligands other than complex **10**. The sum of the angles at N(1) and N(2) of 359.6(5) and 359.9(4)°, respectively, again confirms the trigonal planar nature of these N-atoms when the alkene component is not coordinated to the Ni-atom. The mean P–N and alkene C=C distances are 1.658(4) and 1.329(7) Å, respectively, consistent with the corresponding values in **8**. The mean Ni–P distances for **8** and **10** are 2.154(1) Å

and 2.101(1) Å, respectively, which are similar to those found in **2a** and **2b** and indicate that these distances are not influenced significantly by the modified coordination environment around the Ni-atom, nor by its formal oxidation state.

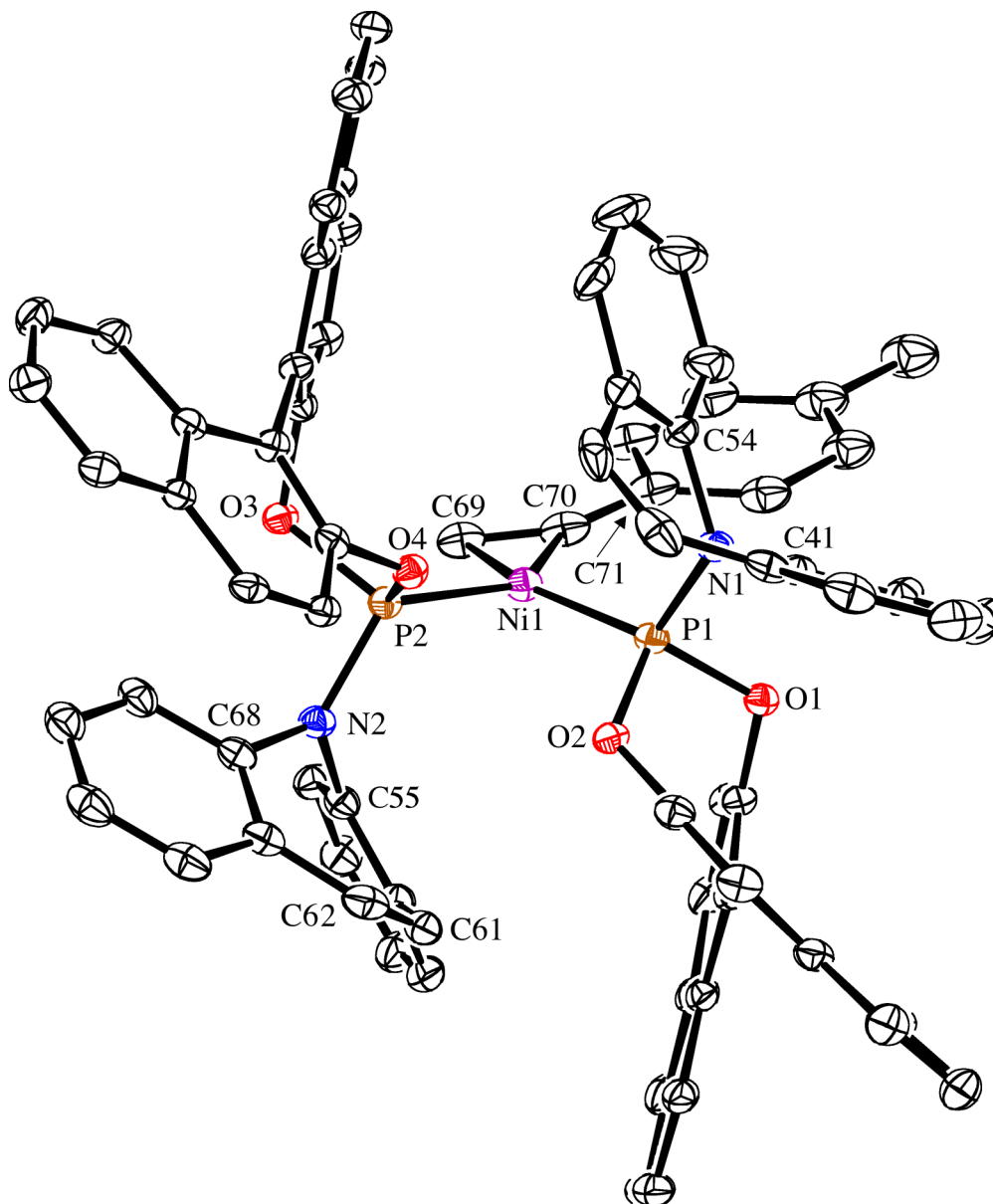


Figure 5. The molecular structure of complex (*S,S*)-**10** in the crystal (50% probability ellipsoids, hydrogen atoms and minor components of the disordered alkyne ligand are omitted). Selected bond lengths (Å) and angles (deg) are: Ni1–P1, 2.1017(11); Ni1–P2, 2.1010(9); Ni1–C69, 1.886(4); Ni1–C70, 1.894(4); C69–C70, 1.265(7); P1–N1, 1.650(3); P1–O1, 1.647(2); P1–O2, 1.633(3); P2–N2, 1.665(3); P2–O3, 1.649(2); P2–O4, 1.629(3); C61–C62, 1.326(6); C47–C48, 1.332(7); P1–Ni1–P2, 101.64(4); P1–Ni1–C69, 155.2(3); P1–Ni1–C70, 117.1(3); P2–Ni1–C69, 102.8(3); P2–Ni1–C70,

141.0(3); C69–Ni1–C70, 39.1(2); Ni1–C69–C70, 70.8(2); Ni1–C70–C69, 70.1(2); C69–C70–C71, 142.4(5); Ni1–C70–C71, 147.4(5); Ni1–P1–N1, 118.62(12); Ni1–P2–N2, 119.88(11); P1–N1–C41, 125.9(2); P2–N2–C55, 118.1(2). Torsion angles ϕ (see text for the definition and Scheme 4) along the P–N vectors: 86.6 (P1–N1), 74.4 (P2–N2).

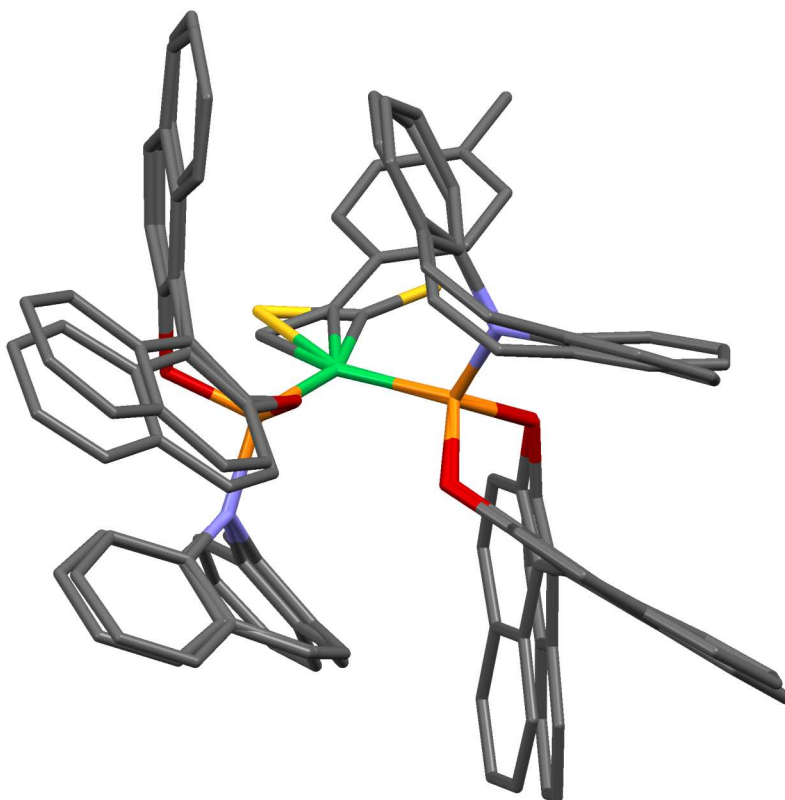
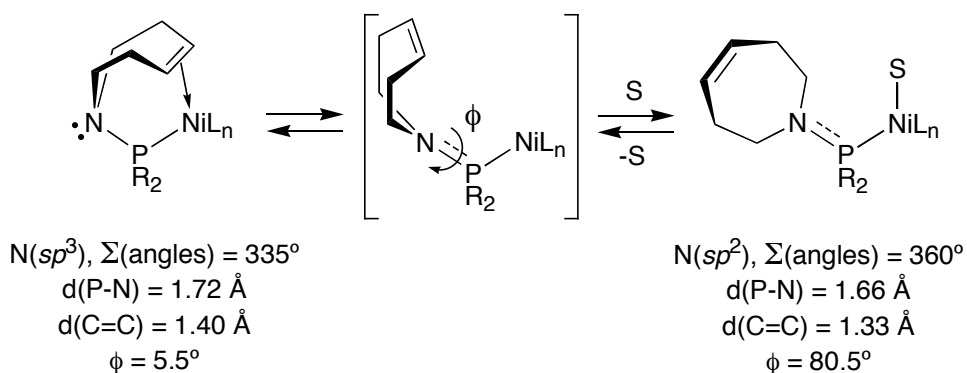


Figure 6. Overlay of the molecular structures of **8** and **10**. Only the major conformation of the disordered 4-ethynyltoluene ligand in **10** is shown.

Scheme 4 depicts the geometrical changes that ligand **5** undergoes on coordination and de-coordination of its alkene arm. The orientation of the alkene ligand is quantified by the torsion angle ϕ around the P–N vector in Ni–P–N \cdots X where X is the mid-point of the alkene C=C bond. When the alkene is coordinated, ideally $\phi = 0$ might be expected, and indeed the values are quite close to zero for **2a** and **2b** (see captions of Figures 1 and 2). When the alkene is not coordinated, the ligand turns through an angle approaching 90° consistently for both ligands in both complexes **8** and **10** (see captions of Figures 3 and 4). The hybridization change of the N atom from sp^3 to sp^2 upon de-coordination of the alkene arm suggests that the bidentate coordination mode of the P,alkene ligands is ‘springloaded’.

Scheme 4. Geometry changes of the P,alkene ligand **5** upon coordination/de-coordination of the alkene function as observed in crystal structures **2a**, **8**, and **10** (mean values, S = substrate molecule, aromatic rings of dibenzazepine omitted for clarity, definition of ϕ : see text)



Three equivalents of 1,2-cyclohexenone, 1,2-cyclopentenone, and coumarine reacted with orange benzene slurries of complex **2a** to afford, by the time of mixing, pale yellow clear solutions of adducts **11a–c** (see Table 2). By contrast, even large excesses of cyclohexanone or benzophenone did not react, and IR spectra of **11a–c** showed the characteristic bands of free C=O functions. This supports the view that only the alkene functions of α,β -unsaturated carbonyl compounds coordinate the Ni center of **2a**. The $^{31}\text{P}\{^1\text{H}\}$ NMR spectra of the *in situ* formed adducts **11a–c** revealed quantitative reactions and were strongly reminiscent of the spectral properties of the dissymmetric complexes **8** and **10** showing characteristic AB quartets. Also, in the ^1H NMR spectra of **11a–c** the characteristic resonances of the coordinated ligand-alkene functions of the starting complex **2a** at δ 5.14 and 5.40 had disappeared. [^1H , ^{31}P] HMQC NMR experiments of **11a–c** identified the two resonances of the α,β -protons of the coordinated enones and coumarine (broad singlets) and confirmed the absence of coordination of the ligand alkene functions. For example, in adduct **11c** the resonances of the α,β -protons of coumarine were shifted strongly up-field to δ 3.90 and 4.21 (br, s) when compared with the pair of doublets at δ 6.4 and 7.7 in free coumarine. The enone adducts **11a** and **11b** showed very similar spectroscopic behavior, and in all cases the integration of the α,β -proton resonances were consistent with the coordination of one sole equivalent of enone per Ni complex. We therefore propose the formation of η^2 adducts of type **11**³⁹ (Table 2) which feature non-stereogenic Ni centers. Unfortunately, these adducts could not be isolated in analytically pure form, because recrystallization, washing with pentane or Et_2O

to eliminate excess enone, or drying under vacuum caused the equilibrium to partially revert to the starting complex **2a**. This reverse reaction formed the same pure (Δ,S,S) diastereoisomer of **2a**. The addition of 3 equiv of 4-ethynyltoluene to the complexes **11a–c** (generated *in situ* with 3 equiv of each of the α,β -unsaturated carbonyl compounds in C_6D_6 solution) led in each case to the quantitative formation of complex **10** in the time of mixing.

Table 2. Reversible coordination of cyclic enones and coumarine to **2a** and characteristic NMR data.

$(\Delta,S,S)\text{-2a}$ + O=C1C=CCCC1 \rightleftharpoons **11**
 (process: recryst./ washings/ vacuum)

adduct	substrate	$^{31}\text{P}\{^1\text{H}\}$ NMR ^a δ^c (ppm); app. J (Hz)	^1H NMR ^b of $\alpha,\beta\text{-H}$, δ^c (ppm)
11a ^d	2-cyclopentenone	151.6 (d), 154.9 (d); 45	3.55, 4.35
11b ^e	2-cyclohexenone	151.4 (d), 159.8 (d); 45	3.23, 4.33
11c ^e	coumarine	155.0 (d), 157.8 (d); 32	3.90, 4.21

^a) 202 MHz; ^b) 500 MHz; ^c) Mayor isomers only (>80% by integration); ^d) THF- D_8 ; ^e) C_6D_6

In conclusion, we have shown that the use of chiral phosphoramidite P,alkene ligands is an excellent method for the high-yield synthesis of optically pure complexes that feature stereogenic Ni(0) centers. **2a** and **2b** are rare examples of stereogenic-at-metal complexes that are not stabilized by $\eta^5\text{-Cp}^-$ or $\eta^6\text{-arene}$ type ligands. Apart from presenting an unambiguous and stable stereochemistry, these novel Ni(0) complexes are air and moisture stable thanks to the protecting hemilabile alkene functions of ligands **5** and **6**, but nonetheless, once dissolved in the appropriate solvent, readily fix and activate small molecules such as CS_2 , alkynes, and α,β -unsaturated carbonyl compounds, the latter reversibly so. The results also indicate that phosphoramidite ancillary ligands form Ni(0) complexes of sufficient electron density to activate small molecules. Structural data of the CS_2 adduct **8**, however, indicate diminished electron density on the Ni center when compared to phosphine stabilized analogues. In contrast, ancillary ligand basicity does not seem to exert great influence on alkyne coordination as observed in adduct **10**. The binding affinity for complex **2a** of the substrates we tested follow the order $\text{CS}_2 > \text{alkynes} > \text{enones}$. Finally, the structural data demonstrate that $[\text{Ni}(\text{P,alkene})_2]$ complexes of

topology **2** can indeed be viewed as latent 14 ve⁻ species **4** (Scheme 1), and the application of such complexes in asymmetric catalysis is the subject of ongoing investigations in our laboratory.

Acknowledgements

We thank Fonacit (Projects S1-2001000851 and G-2005000433) for financial support, Ms. Noelani Cigüela for technical assistance (NMR laboratory at USB), and the University of Zurich for funding the purchase of an Agilent Technologies SuperNova CCD diffractometer.

References

- ¹ Hartwig, J. *Organotransition Metal Chemistry: From Bonding to Catalysis*, **2010**, 1st ed., University Science Books, Sausalito, CA.
- ² For structurally characterized chiral Ni complexes of topology **1**, see: (a) Spielvogel, D. J.; Davis, W. M.; Buchwald, S. L. *Organometallics* **2002**, *21*, 3833; (b) Brunner, T. J.; Blank, N. F.; Moncarz, J. R.; Scriban, C.; Anderson, B. J.; Glueck, D. S.; Zakharov, L. N.; Golen, J. A.; Sommer, R. D.; Incarvito, C. D.; Rheingold, A. L. *Organometallics* **2005**, *24*, 2730. For a racemic complex, see: (c) Göthlich, A. P. V.; Tensfeldt, M.; Rothfuss, H.; Tauchert, M. E.; Haap, D.; Rominger, F.; Hofmann, P. *Organometallics* **2008**, *27*, 2189; For achiral complexes, see: (d) Bach, I.; Pörschke, K.-R.; Proft, B.; Goddard, R.; Kopiske, C.; Krüger, C.; Rufinska, A.; Seevogel, K. *J. Am. Chem. Soc.* **1997**, *119*, 3773; (e) Bennett, B. L.; White, S.; Rodgers, D.; Lau, A.; Roddick, D. M. *J. Organomet. Chem.* **2003**, *679*, 65
- ³ For example, the Ni-catalyzed hydrocyanation of diolefins (DuPont process) needs 15 equiv of phosphite ligand per Ni in order to stabilize the catalyst: Bini, L.; Müller, C.; Vogt, D. *Chem. Commun.* **2010**, *46*, 8325 and references cited therein.
- ⁴ For structurally authenticated Pd and Pt complexes, see: (a) Matsumoto, M.; Yoshioka, H.; Yoshida, T.; Otsuka, S. *J. Am. Chem. Soc.* **1974**, *96*, 3322; (c) Immirzi, A.; Musco, A. *Chem. Comm.* **1974**, 400; (d) Otsuka, S.; Yoshida, T.; Matsumoto, M.; Nakatsu, K. *J. Am. Chem. Soc.* **1976**, *98*, 5850; (e) Fortman, G. C.; Scott, N. M.; Linden, A.; Stevens, E. D.; Dorta, R.; Nolan, P. *Chem. Commun.* **2010**, *46*, 1050; For Ni, see: (f) Arduengo, III, A. J.; Gamper, S. F.; Calabrese, J. C.; Davidson, F. *J. Am. Chem. Soc.* **1994**, *116*, 4391.
- ⁵ (a) Jeffrey, J. C.; Rauchfuss, T. B. *Inorg. Chem.* **1979**, *18*, 2658.
- ⁶ Mariz, R.; Briceño, A.; Dorta, R.; Dorta, R. *Organometallics* **2008**, *27*, 6605.
- ⁷ The stepwise hemilability of such ligands in cationic square planar complexes of the type [Rh^I(P,alkene)₂]⁺ was demonstrated with nitrogen and chloride nucleophiles: Drinkel, E.; Briceño, A.; Dorta, R.; Dorta, R. *Organometallics* **2010**, *29*, 2503. For hemilabile interactions involving chiral ‘monodentate’ phosphoramidite ligands, see: (b) Mikhel, I. S.; Rüegger, H.; Butti, P.; Camponovo, F.; Huber, D.; Mezzetti, A. *Organometallics* **2008**, *27*, 2937.
- ⁸ For a structurally characterized complex of this topology, see: Bennett, A. M.; Chiraratvatana, C.; Robertson, G. B.; Tooptakong, U. *Organometallics* **1988**, *7*, 1394.
- ⁹ For isolated Ni analogues with monodentate ligands that serve as a precursors to d¹⁰-ML₂ synthons, see: (a) Johnson, S. A.; Huff, C. W.; Mustafa, F.; Saliba, M. *J. Am. Chem. Soc.* **2008**, *130*, 17278; (b) Hatnean, J. A.; Beck, R.; Borrelli, J. D.; Johnson, S. A. *Organometallics* **2010**, *29*, 6077.
- ¹⁰ For asymmetric alkene hydrovinylation, see (a) Nomura, N.; Jin, J.; Park, H.; RajanBabu, T. V. *J. Am. Chem. Soc.* **1998**, *120*, 459; (b) Nandi, M.; Jin, J.; RajanBabu, T. V. *J. Am. Chem. Soc.* **1999**, *121*, 9899; (c) Franciò, G.; Faraone, F.; Leitner, W. *J. Am. Chem. Soc.* **2002**, *124*, 736; (d) Hölscher, M.;

Franciò, G.; Leitner, W. *Organometallics* **2004**, *23*, 5606. For asymmetric alkylation of aldehydes and enones, see: (e) Biswas, K.; Chapron, A.; Cooper, T.; Fraser, P. K.; Novak, A.; Prieto, O.; Woodward, S. *Pure Appl. Chem.* **2006**, *78*, 511. For other catalytic Ni systems where hemilabile ligand behavior seems to be crucial, see for example: (f) Hayashi, T.; Konishi, M.; Fukushima, M.; Mise, T.; Kagotani, M.; Tajika, M.; Kumada, M. *J. Am. Chem. Soc.* **1982**, *104*, 180; (g) Hayashi, T.; Hayashizaki, K.; Ito, Y. *J. Am. Chem. Soc.* **1988**, *110*, 8153.

¹¹ Structurally certified Ni-CO₂ complexes are exceedingly rare: Aresta, M.; Nobile, C. F. *J. Chem. Soc., Chem. Commun.* **1975**, 636 and ref. 14(c).

¹² For Ni-catalyzed [2+2+2] additions of CO₂ to alkynes, see: (a) Kreher, U.; Schebesta, S.; Walther, D. *Z. anorg. allg. Chem.* **1998**, *624*, 602; (b) Louie, J.; Gibby, J. E.; Farnworth, M. V.; Tekavec, T. N. *J. Am. Chem. Soc.* **2002**, *124*, 15188.

¹³ (a) Werner, H. *Coord. Chem. Rev.* **1982**, *43*, 165; (b) Ibers, J. A. *Chem. Soc. Rev.* **1982**, *11*, 57; (c) Pandey, K. K. *Coord. Chem. Rev.* **1995**, *140*, 37.

¹⁴ For structural reports, see: (a) Bianchini, C.; Ghilardi, C. A.; Meli, A.; Midollini, S.; Orlandini, A. *J. Chem. Soc., Chem. Commun.* **1983**, 753; (b) Bianchini, C.; Masi, D.; Mealli, C.; Meli, A. *Inorg. Chem.* **1984**, *23*, 2838; (c) Anderson, J. S.; Iluc, V. M.; Hillhouse, G. L. *Inorg. Chem.* **2010**, *49*, 10203.

¹⁵ For CS₂ activation with Ru and Os complexes that are stabilized by secondary F···M interactions, see: Arroyo, M.; Bernès, S.; Cerón, J.; Rius, J.; Torrens, H. *Inorg. Chem.* **2004**, *43*, 986.

¹⁶ For the activation of CS₂ and phenylacetylene with a hemilabile Ru system, see: Lindner, E.; Lin, Y.-C.; Geprägs, M.; Yih, K.-H.; Fawzi, R.; Steimann, M. *J. Organomet. Chem.* **1996**, *512*, 101;

¹⁷ (a) Consiglio, G.; Morandini, F. *Chem. Rev.* **1987**, *87*, 761; (b) Knof, U.; von Zelewsky, A. *Angew. Chem., Int. Ed.* **1999**, *38*, 303; (b) Brunner, H. *Angew. Chem., Int. Ed.* **1999**, *38*, 1194; (c) Fontecave, M.; Hamelin, O.; Ménage, S. *Top. Organomet. Chem.* **2005**, *15*, 271.

¹⁸ Recent examples are: (a) Pinto, P.; Marconi, G.; Heinemann, F. W.; Zenneck, U. *Organometallics* **2004**, *23*, 374; (b) Hintermann, L.; Xiao, L.; Labonne, A.; Englert, U. *Organometallics* **2009**, *28*, 5739; (c) Brunner, H.; Ike, H.; Muschiol, M.; Tsuno, T.; Umegaki, N.; Zabel, M. *Organometallics* **2011**, *30*, 414; (d) Brunner, H.; Ike, H.; Muschiol, M.; Tsuno, T.; Koyama, K.; Kurosawa, T.; Zabel, M. *Organometallics* **2011**, *30*, 3666; (e) Brunner, H.; Muschiol, M.; Tsuno, T.; Ike, H.; Kurosawa, T.; Koyama, K. *Angew. Chem. Int. Ed.* **2012**, *51*, 1067.

¹⁹ (a) Faller, J. W.; Chao, K.-H. *J. Am. Chem. Soc.* **1983**, *105*, 3893; (b) Flood, T. C.; Campbell, K. D.; Downs, H. H.; Nakanishi, S. *Organometallics* **1983**, *2*, 1590; (c) Faller, J. W.; Chao, K.-H. *Organometallics* **1984**, *3*, 927; (d) Davies, S. G. *Pure & Appl. Chem.* **1988**, *60*, 13; (e) Otto, M.; Parr, J.; Slawin, A. M. Z. *Organometallics* **1998**, *21*, 4527; (f) Álvarez, P.; Lastra, E.; Gimeno, J.; Braña, P.; Sordo, J. A.; Gomez, J.; Falvello, L. R.; Bassetti, M. *Organometallics* **2004**, *23*, 2956; (g) Faller, J. W.; Fontaine, P. P. *Organometallics* **2007**, *26*, 1738.

²⁰ (a) Carmona, D.; Lahoz, F. J.; Elipse, S.; Oro, L. A.; Lamata, M. P.; Viguri, F.; Mir, C.; Cativiela, C.; López-Ram de Víu, M. P. *Organometallics* **1998**, *17*, 2986; (b) Brunner, H.; Prommesberger, M. *Tetrahedron: Asymmetry* **1998**, *9*, 3231; (c) Faller, J. W.; Grimmond, B. J.; D'Alliessi, D. G. *J. Am. Chem. Soc.* **2001**, *123*, 2525; (d) Faller, J. W.; Grimmond, B. J. *Organometallics* **2001**, *20*, 2454; (e) Carmona, D.; Lahoz, F. J.; Elipse, S.; Oro, L. A.; Lamata, M. P.; Viguri, F.; Sánchez, F.; Martínez, S.; Cativiela, C.; López-Ram de Víu, M. P. *Organometallics* **2002**, *21*, 5100; (f) Brunner, H.; Zwack, T.; Zabel, M. *Organometallics* **2003**, *22*, 1741; (g) Ghebreyessus, K. Y.; Gül, N.; Nelson, J. H. *Organometallics* **2003**, *22*, 2977; (h) Faller, J. W.; Fontaine, P. P. *Organometallics* **2005**, *24*, 4132.

²¹ For alkene hydrogenation, see: (a) Ohta, T.; Takaya, H.; Kitamura, M.; Nagai, K.; Noyori, R. *J. Org. Chem.* **1987**, *52*, 3176. For related structure reports, see: (b) Ohta, T.; Takaya, H.; Noyori, R. *Inorg. Chem.* **1988**, *27*, 566; (c) Ashby, M. T.; Khan, M. A. *Organometallics* **1991**, *10*, 2011. For imine hydrogenation, see: (d) Uematsu, N.; Fujii, A.; Hashiguchi, S.; Ikariya, T.; Noyori, R. *J. Am. Chem.*

- Soc.* **1996**, 118, 4916. For ketone hydrogenation, see: (e) Matsumura, K.; Hashiguchi, S.; Ikariya, T.; Noyori, R. *J. Am. Chem. Soc.* **1997**, 119, 8738; (f) Haack, K.-J.; Hashiguchi, S.; Fujii, A.; Ikariya, T.; Noyori, R. *Angew. Chem. Int. Ed.* **1997**, 36, 285; (g) Ohkuma, T.; Utsumi, N.; Tsutsumi, K.; Murata, K.; Sandoval, C.; Noyori, R. *J. Am. Chem. Soc.* **2006**, 128, 8724. For hydrogenation of aldehydes, see: (h) Yamada, I.; Noyori, R. *Org. Lett.* **2000**, 2, 3425.
- ²² (a) Linden, A.; Dorta, R. *Acta Crystallogr.* **2010**, C66, m290; For use of **7** as isolated complex, see (b) Roggen, M.; Carreira, E. M. *Angew. Chem. Int. Ed.* **2011**, 50, 5568; For **7** formed *in situ*, see: Lafrance, M.; Roggen, M.; Carreira, E. M. *Angew. Chem. Int. Ed.* **2012**, 51, 3470.
- ²³ (a) Modder, J. F.; Ernsting, J.-M.; Vrieze, K.; de Wit, M.; Stam, C. H.; van Koten, G. *Inorg. Chem.* **1991**, 30, 1208; (b) Brunner, H.; Faustmann, P.; Dietl, A.; Nuber, B. *J. Organomet. Chem.* **1997**, 542, 255 and references cited therein.
- ²⁴ (a) Malcolmson, S. J.; Meek, S. J.; Sattely, E. S.; Schrock, R. R.; Hoveyda, A. H. *Nature* **2008**, 456, 933; (b) Marinescu, S. C.; Schrock, R. R.; Li, B.; Hoveyda, A. H. *J. Am. Chem. Soc.* **2009**, 131, 58; (c) Yu, M.; Ibrahim, I.; Hasegawa, M.; Schrock, R. R.; Hoveyda, A. H. *J. Am. Chem. Soc.* **2012**, dx.doi.org/10.1021/ja210946z.
- ²⁵ Krysan, D. J.; Mackenzie, P. B. *J. Org. Chem.* **1990**, 55, 4229.
- ²⁶ Repeated EAs gave consistently low C values. This is a known problem for Ni-alkyne complexes and is attributed to Ni-carbide formation during combustion (see ref. 36(m)).
- ²⁷ *CrysAlis PRO*, Agilent Technologies: Yarnton, England, **2010**.
- ²⁸ Sheldrick, G. M. *SHELXS97*, *Acta Crystallogr.* **2008**, A64, 112.
- ²⁹ (a) Flack, H. D. *Acta Crystallogr., Sect. A* **1983**, 39, 876; (b) Flack, H. D., Bernardinelli, G. *Acta Crystallogr., Sect. A* **1999**, 55, 908; (c) Flack, H. D., Bernardinelli, G. *J. Appl. Crystallogr.* **2000**, 33, 1143.
- ³⁰ van der Sluis, P.; Spek, A. L. *Acta Crystallogr.* **1990**, A46, 194.
- ³¹ Spek, A. L. *PLATON, Program for the Analysis of Molecular Geometry*, University of Utrecht: The Netherlands, **2010**.
- ³² Work in progress. For a recent example of C-Cl activation and related literature, see: Csok, Z.; Vechorkin, O.; Harkins, S. B.; Scopelliti, R.; Hu, X. *J. Am. Chem. Soc.* **2008**, 130, 8156.
- ³³ (a) Brunner, H. *Eur. J. Inorg. Chem.* **2001**, 905; (b) Faller, J. W.; Parr, J.; Lavoie, A. R. *New J. Chem.* **2003**, 27, 899.
- ³⁴ Linden, A.; Dorta R., unpublished results.
- ³⁵ This represents an alternative, chiral C₁ building-block: Gandhi, T.; Nethaji, M.; Jagirdar, B. R. *Inorg. Chem.* **2003**, 42, 4798.
- ³⁶ For structurally characterized monomeric Ni(0) complexes of di-substituted alkynes, see: (a) Dickson, R. S.; Ibers, J. A. *J. Organometal. Chem.* **1972**, 36, 191; (b) Rosenthal, U.; Oehme, G.; Görls, H.; Burlakov, V. V.; Polyakov, A. V.; Yanovsky, A. I.; Struchkov, Y. T. *J. Organomet. Chem.* **1991**, 409, 299 and references therein; (c) Bartik, T.; Happ, B.; Iglewsky, M.; Bandmann, H.; Boese, R.; Heimbach, P.; Hoffmann, T.; Wenschuh, E. *Organometallics* **1992**, 11, 1235; Walther, D.; Schmidt, A.; Klettke, T.; Imhof, W.; Görls, H. *Angew. Chem. Int. Ed.* **1994**, 33, 1373; (d) Walther, D.; Klettke, T.; Görls, H.; Imhof, W. *J. Organomet. Chem.* **1997**, 534, 129; (e) Edelbach, B. L.; Lachicotte, R. J.; Jones, W. D. *Organometallics* **1999**, 18, 4040; (f) Eisch, J. J.; Xin Ma; Han, K. I.; Gitua, J. N.; Krüger, C. *Eur. J. Inorg. Chem.* **2001**, 77; (g) Müller, C.; Lachicotte, R. J.; Jones, W. D. *Organometallics* **2002**, 21, 1975; (h) Waterman, R.; Hillhouse, G. L. *Organometallics* **2003**, 22, 5182; (f) Weng, Z.; Teo, S.; Hor, T. S. A. *Organometallics* **2006**, 25, 4878; (i) Schaub, T.; Backes, M.; Radius, U. *Organometallics* **2006**, 25, 4196; (k) Ruhland, K.; Obenhuber, A.; Hoffmann, S. D. *Organometallics* **2008**, 27, 3482; (l) ref. 4; (m) Sgro, M. J.; Stephan, D. W. *Dalton Trans.* **2010**, 39, 5786; (n) ref. 9(b); (o) Barrios-Francisco, R.; Benitez-Paez, T.; Flores-Alamo, M.; Arevalo, A.; Garcia, J. J. *Chem. Asian J.* **2011**, 6,

842.

³⁷ (a) Pörschke, K. R.; Tsay, Y.-H.; Krüger, C. *Angew. Chem. Int. Ed.* **1985**, *24*, 323; (b) Bonrath, W.; Pörschke, K. R.; Wilke, G.; Angermund, K.; Krüger, C. *Angew. Chem. Int. Ed.* **1988**, *27*, 833.

³⁸ See for example: Ogata, K.; Atsuumi, Y.; Fukuzawa, S. *Org. Lett.* **2011**, *13*, 122 and references cited therein.

³⁹ For a structurally characterized Ni-adduct of an α,β -unsaturated carbonyl compound, see ref. 36(m).